8-2012

Cr-Hollandite: Breaking Tradition with Todorokite-type Manganese Oxides

Stanton Ching
Connecticut College, sschi@conncoll.edu

Jonathan P. Franklin

Carley M. Spencer

Recommended Citation
Ching, S. S., Franklin, J. P., & Spencer, C. M. Cr-hollandite: Breaking tradition with todorokite-type manganese oxides. *Polyhedron*, **2012**, doi:10.1016/j.poly.2012.07.099

Elsevier Editorial System(tm) for Polyhedron
Manuscript Draft

Manuscript Number: POLY-D-12-00837R1

Title: Cr-Hollandite: Breaking Tradition with Todorokite-type Manganese Oxides

Article Type: Michelle Millar Issue

Keywords: manganese oxide
chromium hollandite
hydrothermal synthesis

Corresponding Author: Dr. Stanton Ching,

Corresponding Author's Institution: Connecticut College

First Author: Stanton Ching

Order of Authors: Stanton Ching; Jonathan P Franklin; Carley M Spencer

Manuscript Region of Origin: USA

Graphical Abstract (synopsis) (for review)

Click here to download high resolution image

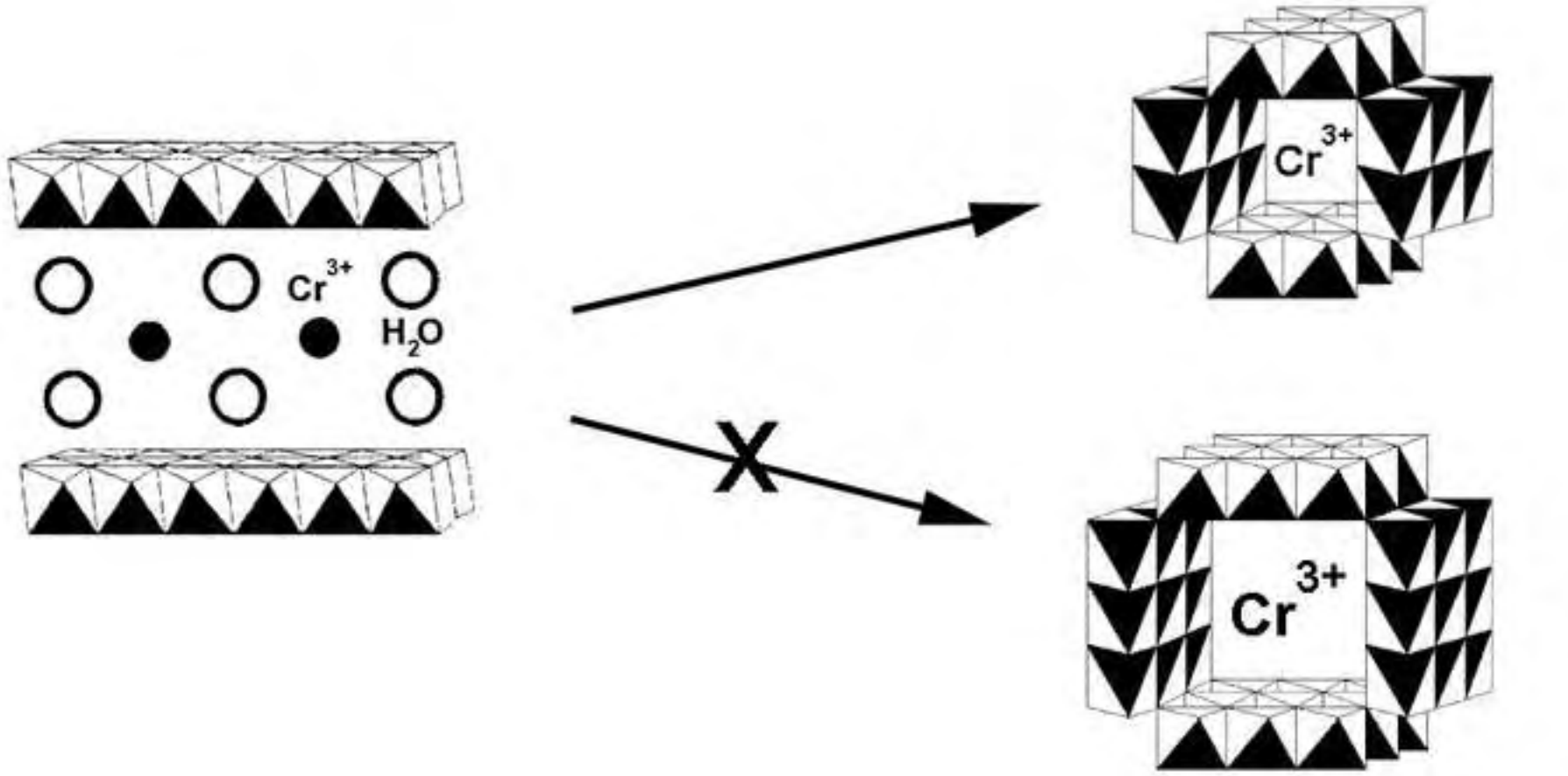

Cr-Hollandite: Breaking Tradition with Todorokite-type Manganese Oxides

Stanton Ching,* Jonathan P. Franklin, and Carley M. Spencer
Department of Chemistry, Connecticut College, New London, CT 06320, USA

* Corresponding author. Tel.: 860-439-2753; fax 860-439-2477; E-mail address: sschi@conncoll.edu

This contribution is dedicated to the memory of Michelle M. Millar, whose talent, generosity, and thoughtfulness touched so many.

ABSTRACT

The synthesis of a tunneled hollandite-type manganese oxide with interstitial and framework Cr^{3+} is described. This unique material is prepared from a layered buserite precursor under conditions previously believed to only yield todorokite-type manganese oxides with larger tunnels. The influence of Cr^{3+} in promoting the hollandite structure has been investigated by selectively placing the cation either in interstitial or framework sites. The use of framework Cr^{3+} in combination with other interstitial cations generates related hollandite and todorokite derivatives. Catalytic oxidation reactions with benzyl alcohol and carbon monoxide have also been examined.

Introduction

Tunneled manganese oxides are interesting and versatile materials with potential applications in heterogeneous catalysis, chemical sensing, hazardous waste remediation, and rechargeable battery technology. [1,2] The most studied of these are hollandite and todorokite, which have frameworks consisting of 2x2 and 3x3 arrangements of edge-shared MnO_6 octahedra, respectively, Fig. 1. Their frameworks are negatively charged due to Mn(III)/Mn(IV) mixed valency and as a result the tunnels play host to cations and water molecules.

The most common hollandite-type manganese oxide is cryptomelane, which has interstitial K^+ serving as a template for the 2x2 tunnels. It can be prepared by a variety of methods, including reflux heating, hydrothermal treatment, and sol-gel processing. [3-5] It is also generated in syntheses of hierarchical urchin-like nanostructured manganese oxides. [6,7] The 3x3 todorokite structure is typically synthesized from layered buserite precursors under hydrothermal conditions. Buserite is a layered manganese oxide with metal cations and water molecules in the inter-lamellar region. Todorokite is typically generated with divalent metals as the templating cation, particularly Mg^{2+} and cations of mid-late first-row transition metals. [8-10] Syntheses of hollandite and todorokite can also be designed for isomorphous doping of metal cations into the manganese oxide framework. [9-12]

In a previous communication, we reported the synthesis under hydrothermal conditions of a hollandite-type manganese oxide with Cr^{3+} in both interstitial and framework locations. [13] The appearance of Cr-hollandite is unique because divalent and trivalent transition metal cations were previously known only as templates for the todorokite structure. [8-10] Here we report further investigation into the formation of Cr-hollandite, including the influence of Cr^{3+} both in tunnel and framework sites, as well as efforts to generate similar materials using other cations. We also examine the catalytic activity of Cr-hollandite in benzyl alcohol and carbon monoxide oxidation reactions.

Material and Methods

Reagent grade chemicals were obtained commercially and used as received. Syntheses of layered birnessite- and buserite-type manganese oxides were based on previously reported procedures.[10] Abbreviations for manganese oxide materials are as follows: birn = birnessite (layered, 7 Å interlayer spacing); buse = buserite (layered, 10 Å interlayer spacing); holl = hollandite (2x2 tunnels); todo = todorokite (3x3 tunnels). Interstitial cations are indicated in front of the material and framework dopants are in parentheses. A designation of (0) indicates absence of framework dopant. For example, Na-birn(Cr) is birnessite with interlayer sodium ion and manganese oxide framework doped with chromium ion; Na-birn(0) is sodium birnessite without framework dopant.

Cr-holl(Cr)

A 1.69-g (10 mmol) sample of $MnSO_4 \cdot H_2O$ was dissolved in 20 mL of water and 30 mL of 6 M NaOH was added slowly with stirring. The resulting tan slurry of $Mn(OH)_2$ was stirred for 10 minutes, then a solid mixture of 1.89 g (7.0 mmol) $K_2S_2O_8$ and 0.37 g (1.4 mmol) $CrCl_3 \cdot 6H_2O$ was added incrementally over 45 minutes. The resulting black slurry was allowed to age for at least one week. The aged sample of Na-birn(Cr) was then filtered, washed 3 times with water, immediately slurried in 50 mL of 0.25 M $Cr(NO_3)_3$, and stirred overnight. The resulting Cr^{3+}-exchanged Cr-buse(Cr) was filtered and washed 3 times with water. The damp Cr-buse(Cr) was loaded into a 30-mL Teflon-lined stainless steel autoclave, slurried with about 15 mL of water, and heated at 160 °C for 1 week. Black Cr-holl(Cr) was isolated by filtration, washed 3 times with water, and dried at 110 °C. A typical yield was 0.5 g.

Cr-holl(0)

Na-birn(0) was prepared, aged, and isolated similarly to Na-birn(Cr) above but without addition of $CrCl_3 \cdot 6H_2O$. Ion exchange was carried out in 20 mL of 1.0 M $Cr(NO_3)_3$ with stirring for 24 h. The resulting Cr-buse(0) was filtered without washing and treated hydrothermally at 160 °C for 1 week. Grey-black Cr-holl(0) was isolated by filtration, washed 3 times with water, and dried at 110 °C.

K-holl(Cr)

By hydrothermal treatment of K-birn(Cr). Na-birn(Cr) was prepared, aged, and isolated as above. Ion exchange was carried out in 50 mL of 1.0 M KNO_3 with stirring overnight. The resulting K-birn(Cr) was filtered, washed 3 times with water, slurried with a 15 mL solution of 0.1 M HCl and 1.0 M KCl, and treated hydrothermally at 160 °C for 1 week. Black K-holl(Cr) was isolated by filtration, washed 3 times with water, and dried at 110 °C.

By calcination of K-birn(Cr). K-birn(Cr) was prepared as above. After drying at 110 °C, the sample was calcined at 500 °C for 2 hours. Black K-birn(Cr) was washed 3 times with water and dried at 110 °C.

M-birn(Cr), M = Mg^{2+}, Fe^{3+}, Ga^{3+}

Ion exchange of Na-birn(Cr) was carried out in 25 mL solutions of 0.25 M metal nitrate with stirring overnight. $Mg(NO_3)_2 \cdot 6H_2O$ and $Fe(NO_3)_3 \cdot 9H_2O$ were used for Mg^{2+} and Fe^{3+}, respectively. Gallium nitrate was obtained with indeterminate waters for hydration, $Ga(NO_3)_3 \cdot xH_2O$, so a value of x=9 was used.

Na-birn(M), M = Mg^{2+}, Fe^{3+}

Na-birnessite(M) was prepared as described for Na-birn(Cr) above, except Mg^{2+} and Fe^{3+} substituted for Cr^{3+} in the same mole quantity using $MgSO_4 \cdot 7H_2O$ and $Fe(NO_3)_3 \cdot 9H_2O$, respectively.

Catalysis with Cr-holl(Cr)

Catalytic oxidation of benzyl alcohol to benzaldehyde was performed in batch mode. A 50-mg sample of Cr-holl(Cr) was slurried with 10 mL of toluene and 1 mmol of benzyl alcohol. The mixture was heated at reflux for 4 hours, after which the catalyst was removed by filtration and the filtrate analyzed by GC-MS.

CO oxidation catalysis was examined in a flow reactor using a 100-mg sample of Cr-holl(Cr) pre-purged at 180 °C in He prior to exposure to the reaction mixture. The catalyst was equilibrated at the experimental temperature in a 1% CO + 1% O_2 in N_2 mixture. Flow was initiated at a space velocity of 35,000 mL/h·$g_{catalyst}$. After 20 minutes, the flow over the catalyst was directed to an online SRI 8610C GC equipped with a silica gel column and TCD detector.

Characterization

Powder X-ray diffraction (XRD) patterns were obtained with a Rigaku Miniflex diffractometer using Cu Kα-radiation. The operating voltage and current were 30 kV and 15 mA, respectively. Scan rates were 2.5 °/min. Sloped backgrounds were observed in low-intensity patterns due to fluorescence by chromium and could not be adequately corrected with background subtraction. Scanning electron microscopy was performed with a LEO 435VP SEM using an acceleration voltage of 20 kV. Energy dispersive analysis with X-rays (EDAX) was performed with an Oxford Instruments EDAX analyzer. Transmission electron microscopy was performed with an FEI Morgagni TEM using an acceleration voltage of 100 kV. Samples were mounted on holey carbon coated Cu grids. Thermogravimetric analyses were carried out using a TA instruments Q50 TGA under a N_2 atmosphere and with a heating rate of 15 °C/min. Total surface areas were determined by BET measurements with a Micromeritics Gemini V surface area analyzer. Elemental analyses of metals were determined by atomic absorption spectroscopy using a Varian 240FS AA. GC-MS was performed with a Hewlett-Packard 5890 GC coupled to a 5971 MSD. Cyclic voltammetry was run on a CH Instruments electrochemical analyzer using carbon paste electrodes with 30% loading of manganese oxide.

Results and Discussion

Cr-holl(Cr)

The synthesis of Cr-hollandite is shown in Scheme 1. XRD and SEM data for Na-birn(Cr) and Cr-buse(Cr) are shown in Figs. 2 and 3, respectively. The XRD pattern of Na-birn(Cr) exhibits weak signals, indicating poor crystallinity even after prolonged aging, Fig. 2(a). By contrast, patterns of Na-birnessite generated without Cr in the framework (Na-birn(0)) were much stronger. Nonetheless, ion exchange with Cr^{3+} produces Cr-buse(Cr) with good crystallinity based on a well-defined XRD pattern, Fig. 2(b). Incorporation of an additional layer of interlamellar water results in the expected peak shift for 7.0 Å interlayer d-spacing in Na-birn(Cr) to 9.6 Å spacing in Cr-buse(Cr). SEM images of both layered materials show the anticipated platelet morphology, Fig. 3. Elemental analyses and TGA measurements give formulas for Na-birn(Cr) and Cr-buse(Cr) of $Na_{0.25}Cr_{0.14}MnO_{2.13}\cdot 0.89H_2O$ and $Cr_{0.32}MnO_{2.24}\cdot 1.24H_2O$, respectively.

Hydrothermal treatment of Cr-buse(Cr) yields hollandite-type manganese oxide with chromium in both interstitial and framework sites, Cr-holl(Cr). Progress of the reaction was monitored by XRD over the course of a week, Fig. 4. The buserite structure is lost within hours, followed by growth of the Cr-holl(Cr) XRD pattern. After two days, the pattern remains relatively unchanged but SEM reveals a thickening of the rod shaped particles across 2-7 days, Fig. 5. SEM and TEM images obtained at earlier stages of the hydrothermal reaction suggest more than one mechanism of particle growth at work, Fig. 6. Striations in the Cr-buse(Cr) platelets resembling wooden floorboards indicate that rod formation occurs by collapse of the layered structure. At the same time, rods exceeding the diameter of the platelets are also observed, suggesting a solid-dissolution-solid growth process that promotes both elongation and thickening of the rods. Both processes have been proposed for the formation of tunneled manganese

oxides from layered structures. [10,14-16] In this system, it appears the layered structure initially collapses to form tunnels around the Cr^{3+} template, resulting in platelet conversion into rods. The solid-dissolution-solid process then takes place with lateral growth being favored over elongation.

The formation of Cr-holl(Cr) is unique. Layered buserites with interlayer transition-metal cations were previously known only as precursors for todorokites. [8-10] Hollandites with interstitial transition metals are obtainable through ion exchange of K^+ in cryptomelane, but these substitution reactions are incomplete. [17,18] Indeed, only one other purely transition-metal hollandite, Ag-hollandite, has been reported to date [19-21] and none are known with transition-metal cations having charges greater than 1+.

Elemental analysis, EDAX, and TGA were used to determine a composition of $Cr_{0.30}MnO_{2..4}$ for Cr-holl(Cr). Analyses of the layered precursors give Cr:Mn ratios of 0.14 for Na-birn(Cr) and 0.32 for Cr-buse(Cr). Thus the formula of Cr-buse(Cr) can be written as $Cr_{0.16}(Cr_{0.14}Mn)O_{2.4}$ to express the distribution of Cr^{3+} in tunnel and framework sites. Loss of chromium in the hydrothermal conversion of Cr-buse(Cr) to Cr-holl(Cr) is supported by the detection of chromium in the aqueous supernatant after reaction. Direct measurement of the Mn oxidation state by redox titration was not carried out because Cr-doped manganese oxides do not suitably dissolve for analysis. However, a value of 3.9 can be calculated from the analytical data that was used to determine the chemical formula. TGA reveals a lack of interstitial water, which is common in hollandite type manganese oxides, Fig. 7. The weight loss of 8% from 350-560 °C is due to oxygen evolution and concomitant formation of the Mn_2O_3 structure. Subsequent 4% loss from 560-630 °C corresponds to formation of the Mn_3O_4 structure. Surface area analysis by BET gives a value of 37 m^2/g, which is below the range of 50-250 m^2/g typically cited for cryptomelane materials. [1] This can be attributed to the morphological preference of Cr-holl(Cr) for thick rods instead of more commonly observed needles and fibers.

Cr-Holl(0)

To investigate the influence of Cr in the manganese oxide framework sites, layered precursors Na-birn(0) and Cr-buse(0) were prepared without isomorphous doping of Cr^{3+} in the layers. This resulted in a difficult conversion of Cr-buse(0) into Cr-holl(0). Week-long hydrothermal treatment of Cr-buse(0) yielded poorly crystalline hollandite, Fig. 8. Crystallinity was not noticeably improved with longer reaction times and higher temperatures. SEM images reveal fibrous morphologies, with regions of needles and long wires, Fig. 9. So despite a poorly crystallized hollandite structure in the absence of framework Cr^{3+}, the morphology of Cr-holl(0) is well defined. The preference to form needles and wires is typical of cryptomelane and other hollandite-type manganese oxides, but contrasts the thicker Cr-holl(Cr) rods obtained when Cr^{3+} is present as part of the tunnel framework. The relatively low surface area of 33 m^2/g and lack of interstitial water as measured by TGA are same characteristics to Cr-holl(Cr). The analyzed formula of Cr-holl(0) was determined to be $Cr_{0.18}MnO_{2.2}$. In comparing the crystallinity and morphology of Cr-holl(0) vs. Cr-holl(Cr), it appears that framework doping of Cr^{3+} facilitates formation of the 2x2 hollandite tunnel structure but inhibits lengthening of the nanorods into needles and wires.

Other Hollandite and Todorokite Derivatives

To further investigate the importance of framework and interstitial Cr^{3+} in tunneled manganese oxides, reactions were investigated using other cations commonly found in synthetic hollandites and todorokites. Given the prevalence of cryptomelane (K-holl) in hollandite chemistry, K-holl(Cr) was targeted to ascertain if Cr^{3+} as a framework dopant would have a disruptive effect on tunnel formation. Calcination of K-birnessite is a known synthetic route to cryptomelane [3,22] so similar treatment was applied to K-birn(Cr) after preparation by ion exchange with Na-birn(Cr). Heating at 500 °C for 2 h produced crystalline K-holl(Cr), demonstrating that framework Cr^{3+} does not affect the formation of 2x2 hollandite with interstitial K^+. This was confirmed by XRD, Fig. 10. SEM images reveal nanorods that

are much smaller than those of Cr-holl(Cr) and Cr-holl(0), Fig. 11. K-holl(Cr) can also be obtained by hydrothermal treatment of a K-birn(Cr) slurry in 0.1 M HCl/1 M KCl for one week at 160 °C. Acidic conditions are conducive to hollandite formation [3] and excess potassium ion minimizes proton exchange during the reaction. The morphology is similar to that of K-holl(Cr) from calcination. The two routes also yield similar compositions. K-holl(Cr) obtained by calcination of K-birn(Cr) has a formula of $K_{0.20}Cr_{0.13}MnO_{2.28}$ while K-holl(Cr) synthesized via hydrothermal treatment analyzed as $K_{0.16}Cr_{0.16}MnO_{2.27}$.

The influence of framework Cr^{3+} was also examine on a todorokite synthesis using Mg-buse(Cr) under hydrothermal conditions. Mg^{2+} is a common tunnel cation in synthetic todorokites, starting from Mg-buserite as a layered precursor. Mg-buse(Cr) is readily prepared by ion exchange of Na-birn(Cr) with $Mg(NO_3)_3$ and subsequent hydrothermal treatment generates Mg-todo(Cr) with an analyzed formula of $Mg_{0.16}Cr_{0.14}MnO_{2.20}\cdot 0.63H_2O$. The XRD patterns of Mg-buse(Cr) and Mg-todo(Cr) are shown in Fig. 12. As reported by our group and others, these patterns are similar. [9,10,23,24] TEM images show a mixture of rods and platelets, Fig. 13, which has been observed in other todorokite systems. [10,24,25] However, in this system the particle sizes are considerably smaller and the rod shapes are more blunt. This is consistent with the influence of Cr^{3+} as a framework dopant in Cr-holl(Cr), Fig. 5. Mg-todo(Cr) also displays a cyclic voltammetric response in a carbon paste composite that is absence with Mg-buse(Cr), [10] with broad cathodic and anodic peaks being observed at -0.72 and +0.07 V respectively vs. SCE. Another Mg-todo(Cr) material was recently synthesized by reacting $Mn(CH_3COO)_2$ and K_2CrO_4 in the presence of $Mg(CH_3COO)_2$ under aqueous reflux. [26] The procedure incorporates even higher levels of Mg^{2+} and Cr^{3+} according to the published formula of $Mg_{0.23}Cr_{0.35}Mn_{0.65}O_{2.05}\cdot xH_2O$. [26]

In addition to serving an interstitial cation, Mg^{2+} has been employed as an isomorphous dopant in the todorokite framework to stabilize the 3x3 tunnel structure. [9,10] Synthetic attempts were therefore made at Cr-buse(Mg) to see if framework Mg^{2+} would exert a similar stabilizing effect in the presence of interstitial Cr^{3+} and to determine if a preference would emerge for the hollandite or todorokite structure. However, hydrothermal treatment of Cr-buse(Mg) gave no reaction.

Syntheses of K-holl(Cr) and Mg-todo(Cr) are not altogether surprising. In hollandites, K^+ is known as an excellent template for the 2x2 tunnel structure, both with and without foreign cation dopants in the manganese oxide framework. Mg^{2+} is a similarly effective template for the 3x3 todorokite system. However, the inhibiting effect of framework Mg^{2+} in attempts to generate tunneled structures with interstitial Cr^{3+} was unexpected. Indeed, with interstitial Cr^{3+} now established in hollandites and framework Mg^{2+} being well known in todorokites, it was predicted that one of the two tunneled materials, Cr-holl(Mg) or Cr-todo(Mg), would be obtained. But in fact the presence of interstitial Cr^{3+} and framework Mg^{2+} together in the same system promotes neither.

Syntheses of Fe- and Ga-hollandites were also investigated, given the closeness of Fe^{3+} and Ga^{3+} in size and charge to Cr^{3+}. Buserites with Fe^{3+} and Ga^{3+} as interlayer occupants or framework dopants were examined to determine if these materials would likewise serve as precursors to hollandite-type manganese oxide. However, this proved not to be the case. Buserites with Fe^{3+} in combination with Cr^{3+} were prepared as Fe-buse(Cr) and Cr-buse(Fe) and these materials were hydrothermally treated similar to Cr-buse(Cr). In the case of Fe-buse(Cr), a weakly diffracting product was obtained with XRD peaks at 2.41, 2.12, and 1.64 Å, which most closely resembled the pattern of the MnO_2 polymorph, akhtenskite (PDF#33-0820). With Cr-buse(Fe), the only crystalline product represented in the XRD pattern had peaks at 4.38, 2.51, 2.39, and 1.85 Å, corresponding to $HCrO_2$ (PDF#33-0600), with no crystalline manganese oxide phase being detected. Buserite with interlayer Ga^{3+} was prepared, Ga-buse(Cr), but this material was unresponsive to hydrothermal treatment. Efforts to dope Ga^{3+} into layered frameworks of birnessite and buserite were unsuccessful, yielding only amorphous material by XRD and little or no detection of Ga by EDAX.

Influence of Cr^{3+} on Hollandite Formation

Synthetic efforts at Cr-hollandite using Cr-buse(Cr), Cr-buse(0), and Cr-buse(Mg) as precursors reveal the importance of framework Cr^{3+} in promoting the 2x2 tunnel structure. With interstitial Cr^{3+} being constant in all three cases: 1) the presence of framework Cr^{3+} led to crystalline Cr-holl(Cr); 2) its absence resulted in poorly crystalline Cr-holl(0), and 3) substitution of Mg^{2+} as the framework dopant failed to produce any tunneled manganese oxide. In addition, the ready formation of K-holl(Cr) from K-birn(Cr) via calcination and hydrothermal treatment demonstrates that framework Cr^{3+} does not interfere with established synthetic routes to hollandite. The lack of tunnel formation with framework Mg^{2+} and interstitial Cr^{3+} is particularly interesting given the proven utility of framework Mg^{2+} in todorokite syntheses and interstitial Cr^{3+} in hollandite preparation.

Interstitial Cr^{3+} plays a necessary role in Cr-hollandite formation. Efforts to synthesize hollandites with other trivalent cations such as Fe^{3+} and Ga^{3+} were unsuccessful despite their identical charge and similar ionic radii. (For coordination number 6: Cr^{3+}, 0.615 Å; Fe^{3+} 0.645 Å; Ga^{3+}, 0.62 Å. [27]) So while Cr-holl(Cr) is readily synthesized, Fe-holl(Cr) and Ga-holl(Cr) have thus far been unattainable. Hydrothermal treatment of their buserite precursors yields non-porous oxide materials or no reaction. When a divalent cation (Mg^{2+}) is substituted for interstitial Cr^{3+} in the buserite precursor, Mg-buse(Cr), hydrothermal treatment produces the expected Mg-todo(Cr). [8-12]

Catalysis

Manganese oxides are a well-known class of catalytic materials. Hollandite-type manganese oxides in particular have attracted considerable interest for oxidation reactions. The ability of Cr-holl(Cr) to promote oxidation reactions was therefore investigated to assess the influence of chromium ion on hollandite catalytic activity. In converting benzyl alcohol to benzaldehyde, the material is moderately active. Reactions carried out in refluxing 0.1 M solutions of benzyl alcohol in toluene with Cr-holl(Cr) resulted 40-50% conversion after 4 h. These results are in the range of moderate to high catalytic activity in cryptomelane (K-hollandite) for the same reaction. [28,29] Glaser and co-workers found catalytic oxidation of benzyl alcohol by cryptomelane to be directly correlated with surface area. [28] Based on these results, the relatively low surface area of 37 m^2/g for Cr-holl(Cr) suggests a mild enhancement of catalytic activity due to the presence of Cr^{3+}. Suib and co-workers established a more effective approach to increased activity by substituting protons for potassium ions in cryptomelane. [29]

Cr-holl(Cr) was also examined as a catalyst for CO oxidation. Conversions to CO_2 of 45-50% were achieved at 200 °C. These results do not improve on the performance of cryptomelane as a CO oxidation catalyst. [30,31]

Conclusions

Chromium(III) ion uniquely promotes the formation 2x2 tunneled hollandite-type manganese oxide from layered buserite precursors. It plays a crucial role both as an interstitial cation and an isomorphous framework dopant. Interstitial Cr^{3+} can be replaced by K^+ and Mg^{2+} to prepare K-hollandite (cryptomelane) and Mg-todorokite with Cr^{3+} remaining in the framework, demonstrating that isomorphous doping of Cr^{3+} does not hinder established reactions of tunneled manganese oxides. However, attempts to generate the hollandite structure by replacing Cr^{3+} with other trivalent cations such as Fe^{3+} and Ga^{3+} were unsuccessful despite identical charge and similar ionic radii. The reason behind this unique chemistry with Cr^{3+} remains unclear. Cr-holl(Cr) is a modest oxidation catalyst for benzyl alcohol and carbon monoxide.

Acknowledgments

David A. Kriz is acknowledged for carrying out the CO oxidation measurements in the labs of Professor Steven L. Suib at the University of Connecticut. J.P.F and C.M.S. acknowledge summer research support from the Keck Foundation.

References

[1] S.L. Suib, J. Mater. Chem. 16 (2008) 1623.
[2] Q. Feng, H. Kanoh, K. Ooi, J. Mater. Chem. 9 (1999) 319.
[3] R. N. DeGuzman, Y.F. Shen, E.J. Neth, S.L. Suib, C.L. O'Young, S. Levine, J.M. Newsam Chem. Mater. 6 (1994) 815.
[4] G. Qiu, H. Huang, S. Dharmarathna, E. Benbow, L. Stafford, S.L. Suib Chem. Mater. 23 (2011) 3892.
[5] S. Ching, J. Roark, N. Duan, S.L. Suib Chem. Mater. 9 (1997) 750.
[6] N. Wang, Y. Gao, J. Gong, X. Ma, X. Zhang, Y. Guo, L. Qu Eur. J. Inorg. Chem. 24 (2008) 3827.
[7] B. Li, G. Rong, L. Huang, C. Feng Inorg. Chem. 45 (2006) 6404.
[8] D.C. Golden, C.C. Chen, J.B. Dixon Science 231 (1986) 717.
[9] Y.F. Shen, S.L. Suib, C.L. O'Young J. Am. Chem. Soc. 116 (1994) 11020.
[10] S. Ching, K.S. Krukowska, S.L. Suib Inorg. Chim. Acta 294 (1999) 123.
[11] J. Cai, J. Liu, W.S. Willis, S.L. Suib Chem. Mater. 13 (2001) 2413.
[12] G.G. Xia, Y.G. Yin, W.S. Willis, J.Y. Wang, S.L. Suib J. Catal. 185 (1999) 91.
[13] S. Ching, P.F. Driscoll, K.S. Kieltyka, M.R. Marvel, S.L. Suib Chem. Commun. (2001) 2486.
[14] C.C. Chen, D.C. Golden, J.B. Dixon Clays Clay Miner. 34 (1986) 565.
[15] Y.F. Shen, S.L. Suib, C.L. O'Young J. Catal. 161(1996) 115.
[16] E. Nicholas-Tolentino, Z.R. Tian, H. Zhou, G. Xia Chem. Mater. 11 (1999) 1733.
[17] M. Tsuji, Y. Tanaka J. Mater. Res. 16 (2001) 108.
[18] L. Li, D.L. King Chem. Mater. 17 (2005) 4335.
[19] F.M. Chang, M. Jansen Angew. Chem. Int. Ed. Engl. 23 (1984) 906.
[20] L. Li, D.L. King Chem. Mater. 17 (2005) 4335.
[21] S. Zhu, A.C. Marschilok, C.Y. Lee, E.S. Takeuchi, K.J. Takeuchi Electrochem. Solid State Lett. 13 (2010) A98.
[22] S. Ching, D.J. Petrovay, M.L. Jorgensen, S.L. Suib Inorg. Chem. 36 (1997) 883.
[23] X.H. Feng, W.F. Tan, F. Liu, J.B. Wang, H.D. Ruan Chem. Mater. 16 (2004) 4330.
[24] H. Cui, X. Feng, W. Tan, J. He, R. Hu, F. Liu Microporous Mesoporous Mater. 117 (2009) 41.
[25] B. Vileno, Y. Ma, H. Zhou, S.L. Suib Microporous Mesoporous Mater. 20 (1998) 3.
[26] H.J. Cui, J.W. Shi, F. Liu, M.L. Fu J. Mater. Chem. 21 (2011) 18527.
[27] R.D. Shannon Acta Crystallogr. A 32 (1976) 751.
[28] F. Schurz, J.M. Bauchert, T. Merker, T. Schleid, H. Hasse, R. Glaser Appl. Catal. A 355 (2009) 42.
[29] Y.C. Son, V.D. Makwana, A.R. Howell, S.L. Suib Angew. Chem. Int. Ed. Engl. 40 (2001) 2480.
[30] S. Liang, F. Teng, G. Bulgan, R. Zong, Y. Zhu J. Phys. Chem. C 112 (2008) 5307.
[31] W.Y. Hernandez, M.A. Centeno, F.R. Romero-Sarria, S. Ivanova, M. Montes, J.A. Odriozola Catal. Today 157 (2010) 160.

Figure Captions

Fig. 1 Structures of tunneled manganese oxides: 2x2 hollandite and 3x3 todorokite.

Fig. 2. XRD patterns and d-spacings for (a) Na-birn(Cr) and (b) Cr-buse(Cr).

Fig. 3. SEM images of (a) Na-birn(Cr) and (b) Cr-buse(Cr).

Fig. 4 XRD patterns of Cr-holl(Cr) at different hydrothermal reaction times. The peaks can be indexed against tetragonal cryptomelane (PDF #42-1348).

Fig. 5 SEM images of Cr-buse(Cr) after (a) 2 days and (b) 7 days.

Fig. 6 (a) SEM and (b) TEM images of Cr-holl(Cr) formation after 8 h of reaction.

Fig. 7 TGA of Cr-holl(Cr).

Fig. 8 XRD pattern of Cr-holl(0).

Fig. 9 SEM images of Cr-holl(0). (a) region displaying needles; (b) region displaying nanowires. Note the change in scale bar.

Fig. 10 XRD pattern of K-holl(Cr).

Fig. 11 SEM images of K-holl(Cr) prepared from K-birn(Cr): (a) by calcination; (b) by hydrothermal treatment.

Fig. 12 XRD patterns and d-spacings for (a) Mg-buse(Cr) and (b) Mg-todo(Cr).

Fig. 13 TEM image of Mg-todo(Cr).

Scheme 1. Synthesis of Cr-holl(Cr).

Figure 1

Click here to download high resolution image

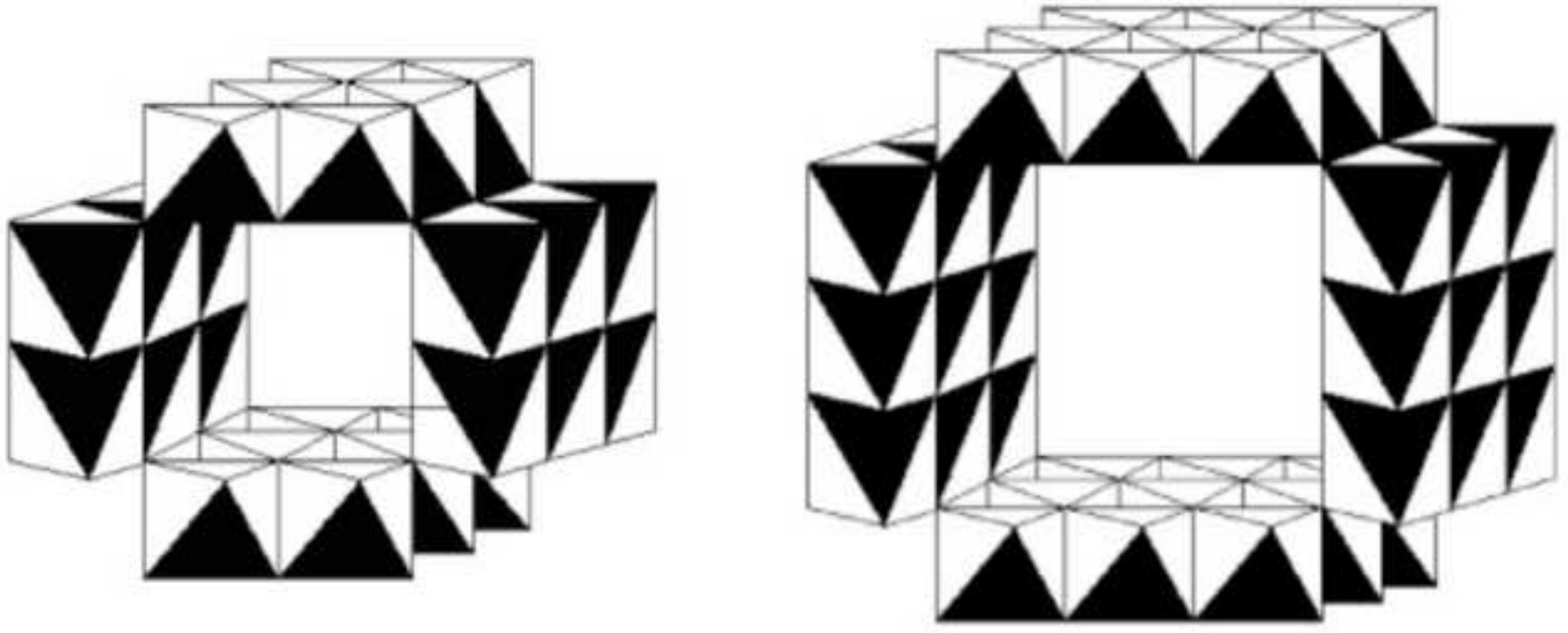

Figure 2

Click here to download high resolution image

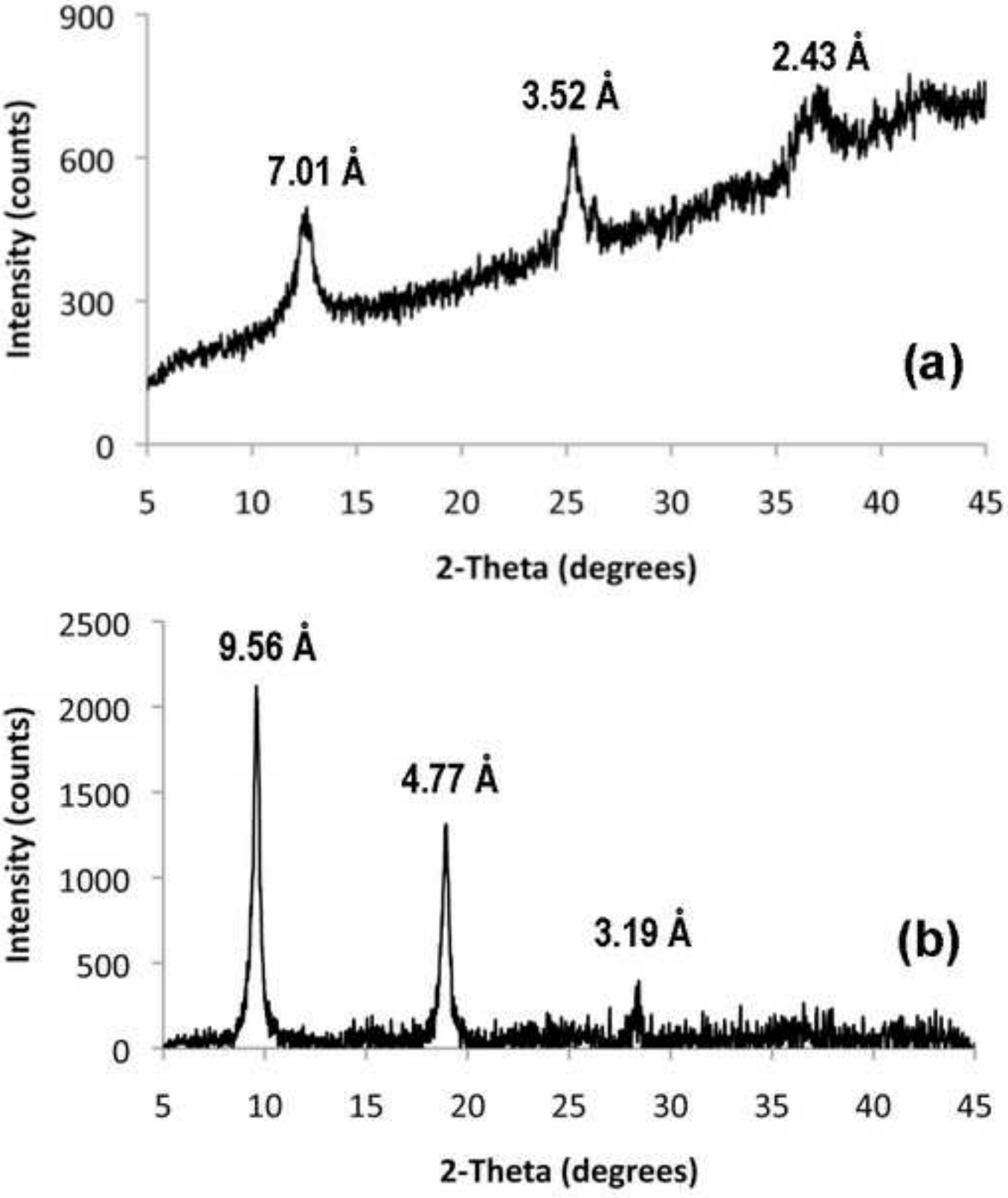

Figure 3

Click here to download high resolution image

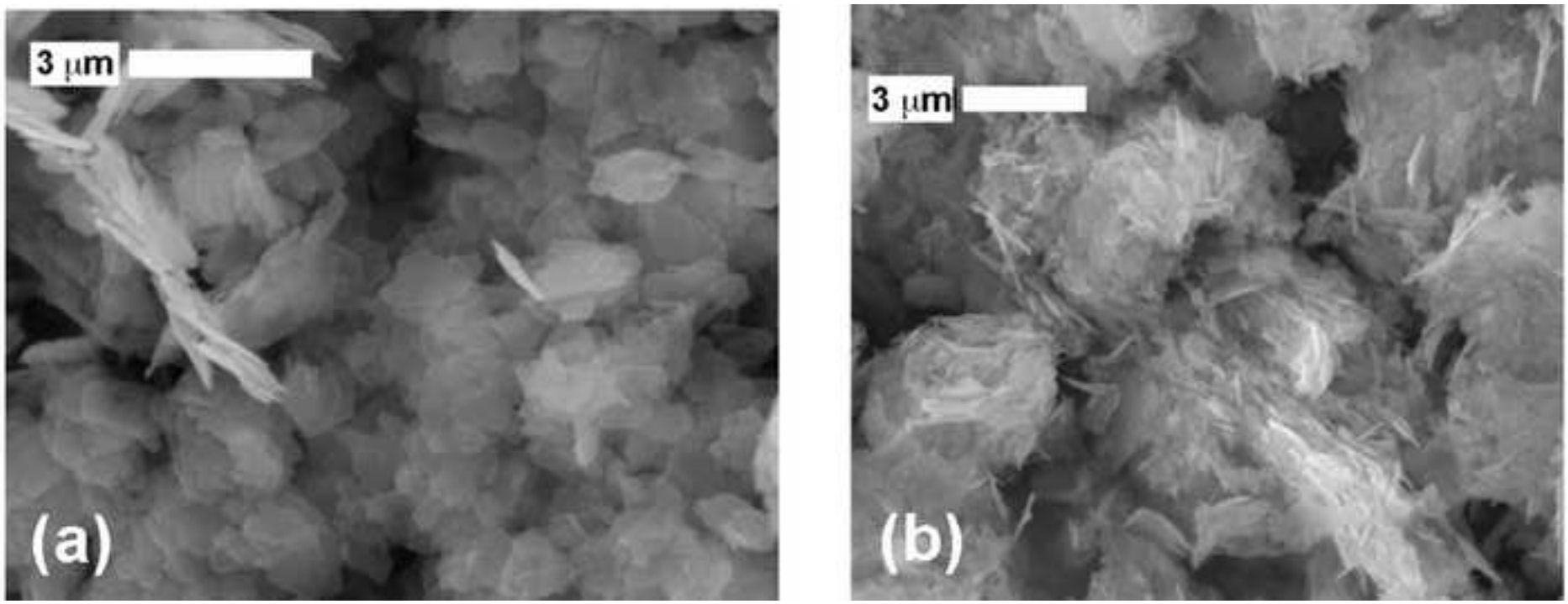

Figure 4

Click here to download high resolution image

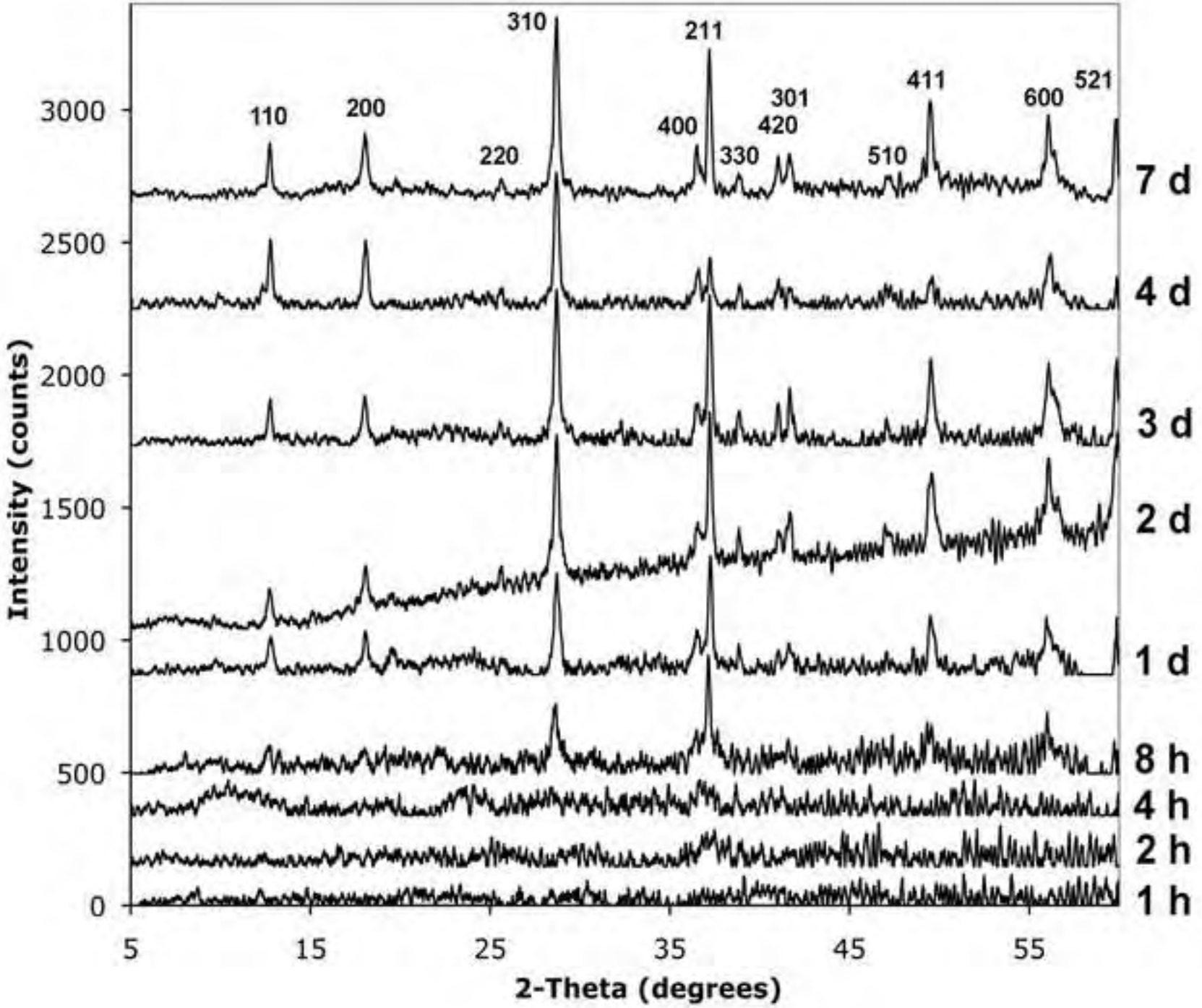

Figure 5

Click here to download high resolution image

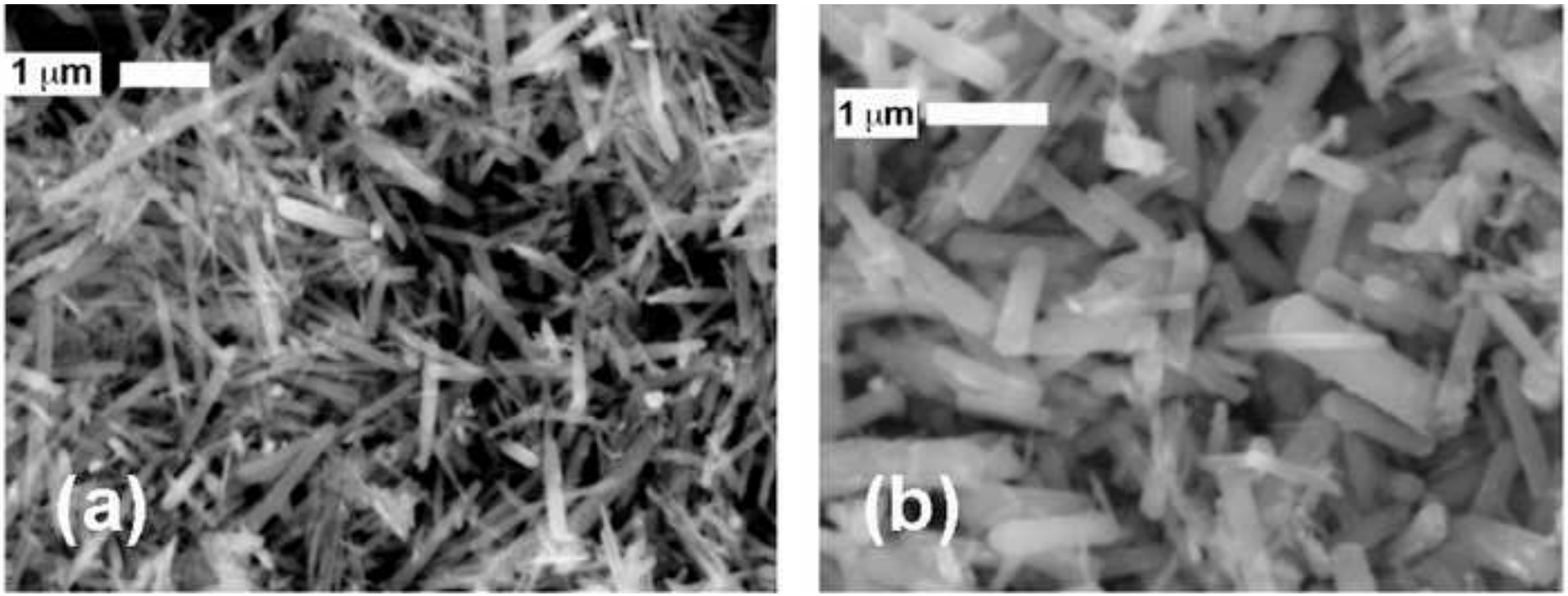

Figure 6
Click here to download high resolution image

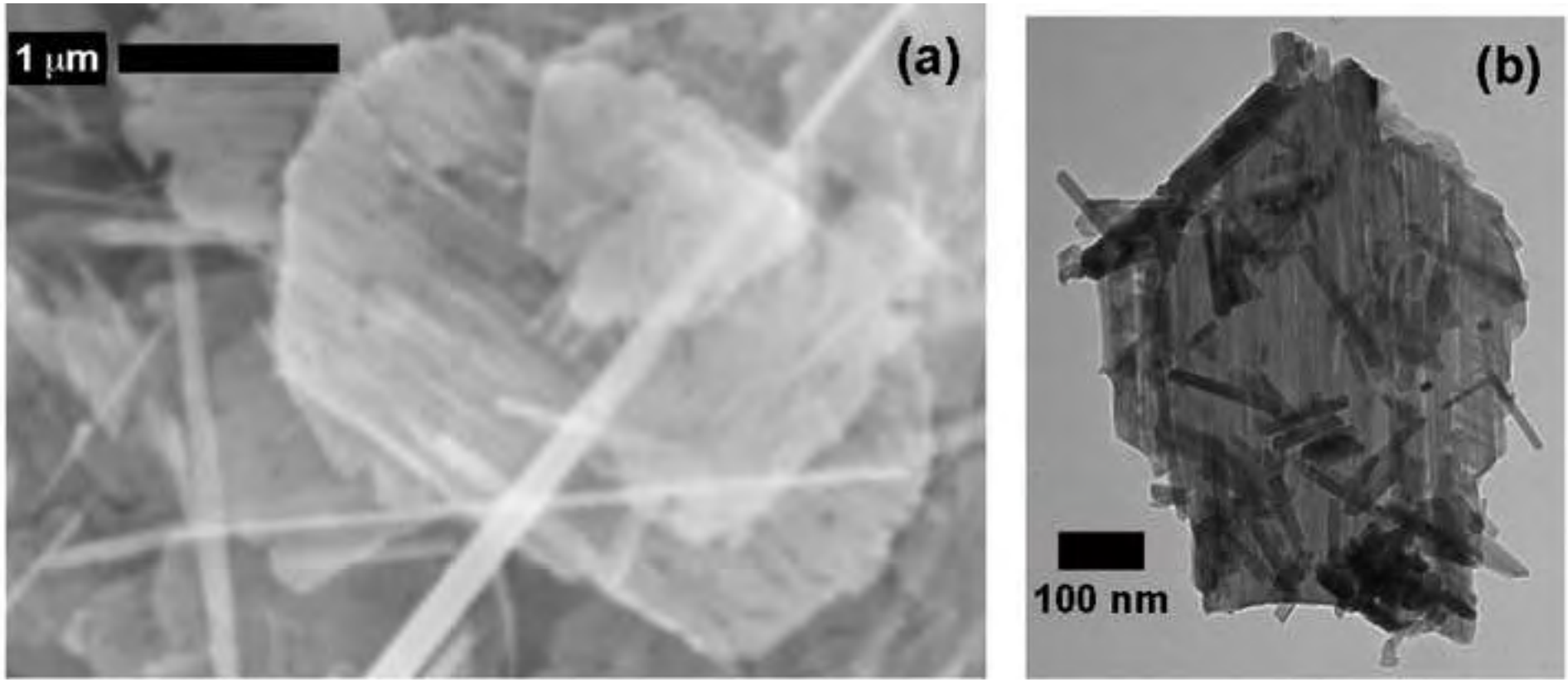

Figure 7

Click here to download high resolution image

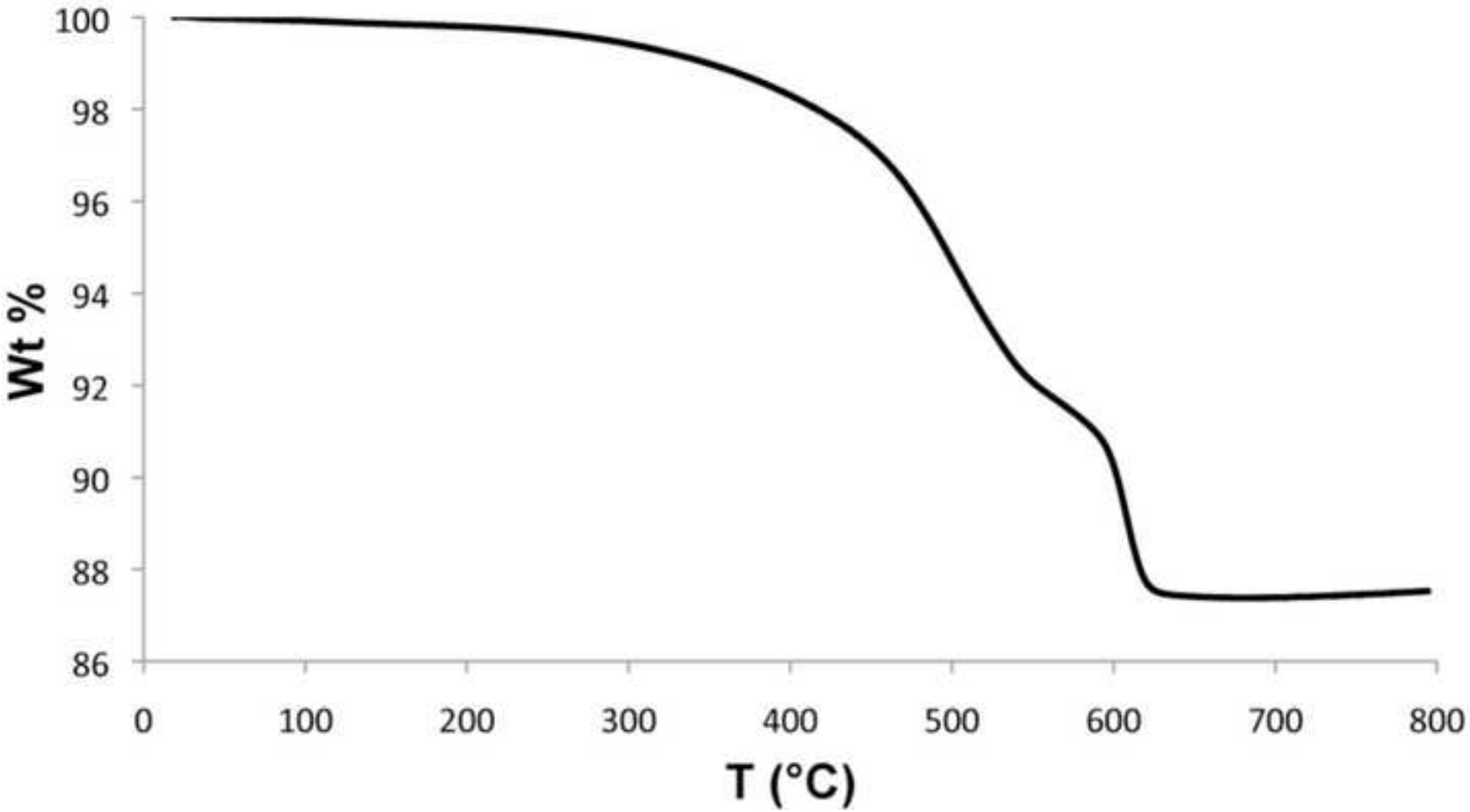

Figure 8

Click here to download high resolution image

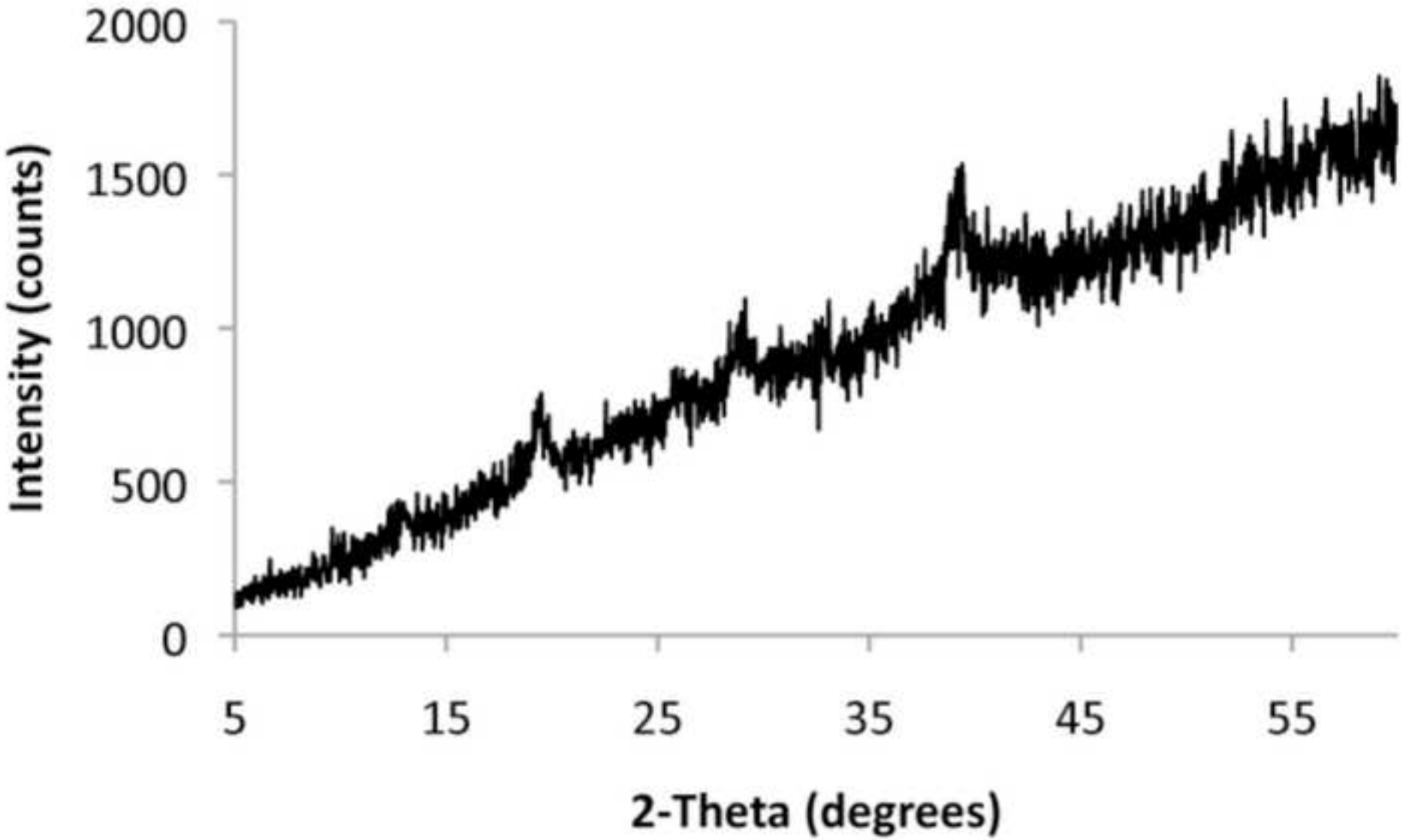

Figure 9

Click here to download high resolution image

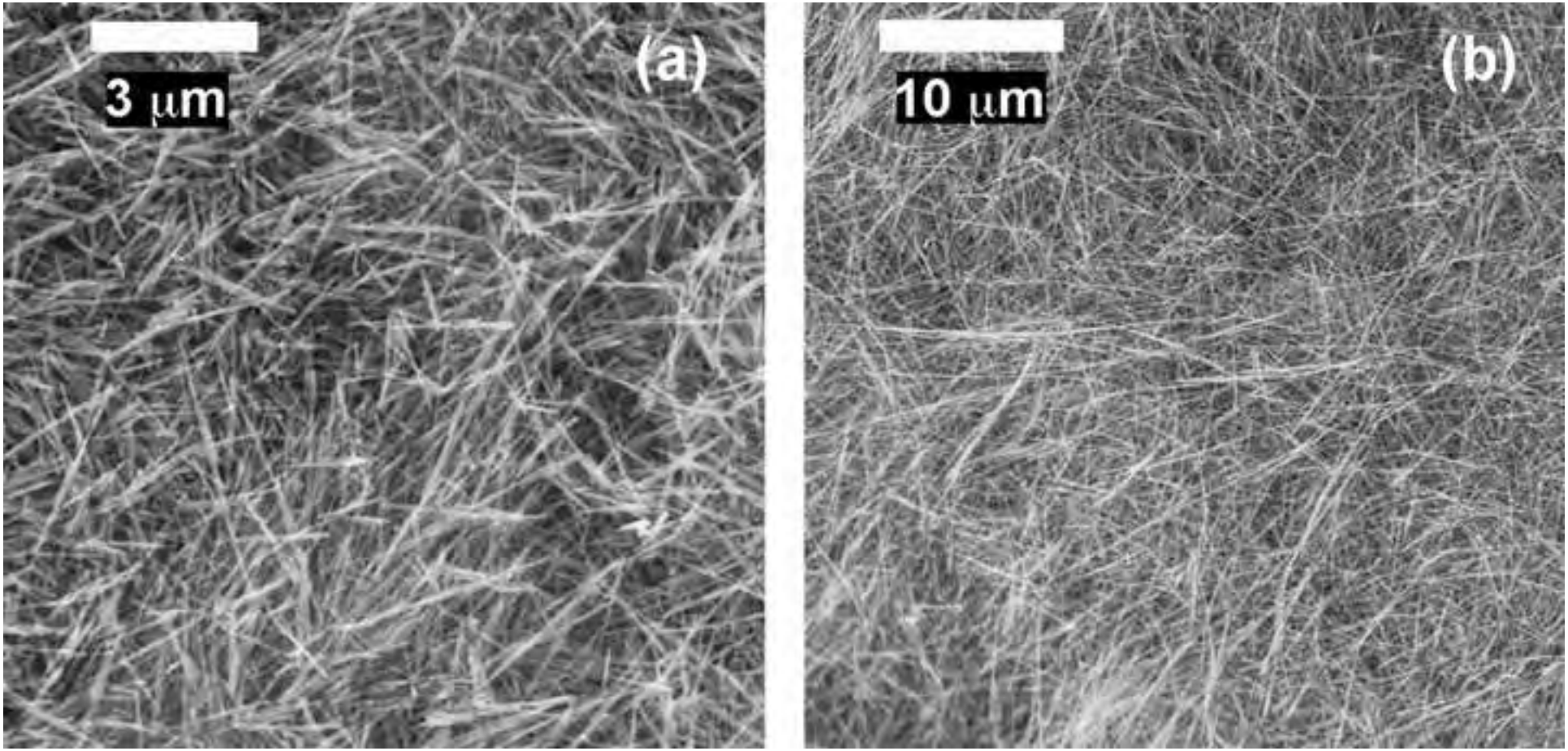

Figure 10

Click here to download high resolution image

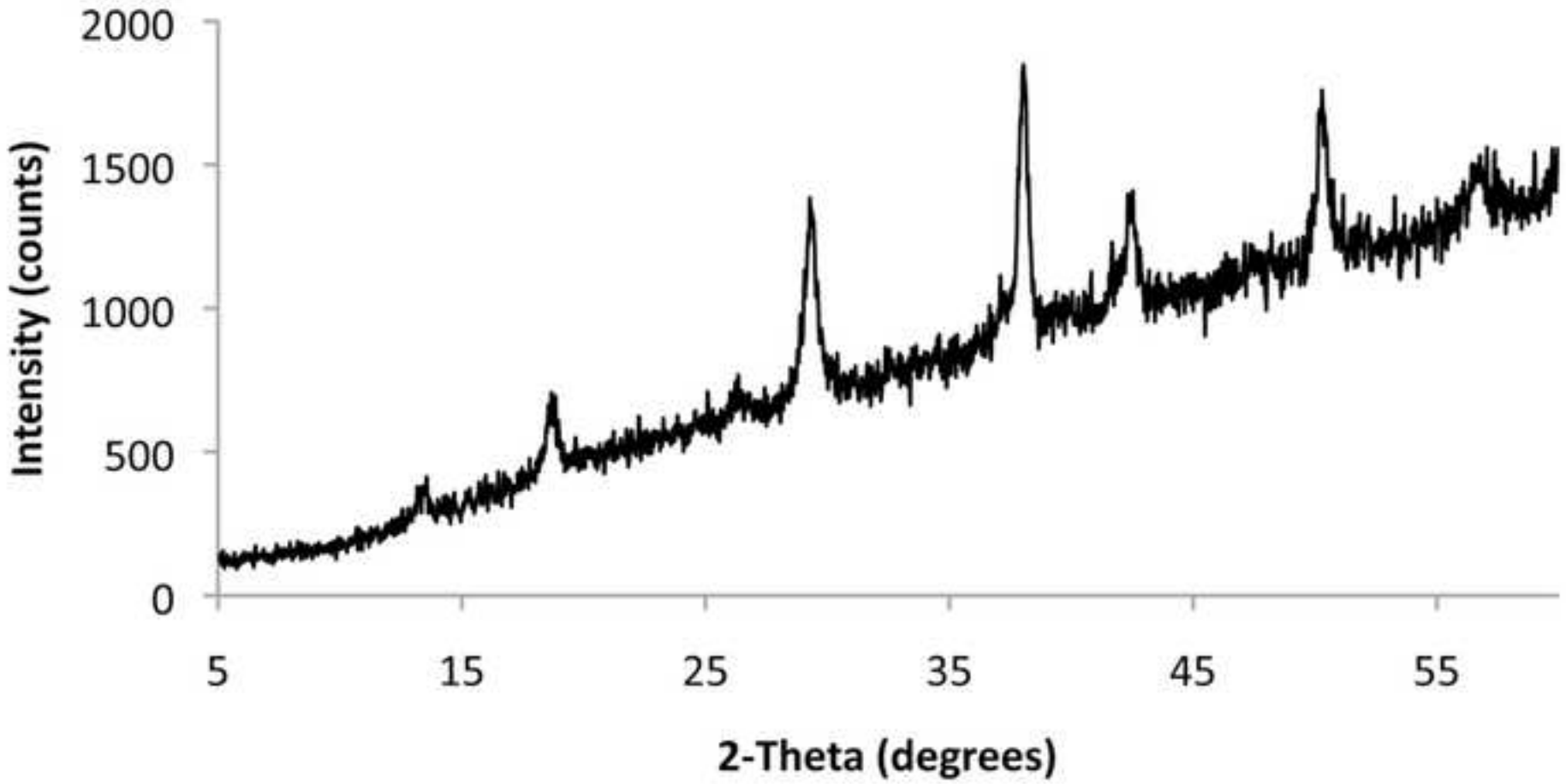

Figure 11
Click here to download high resolution image

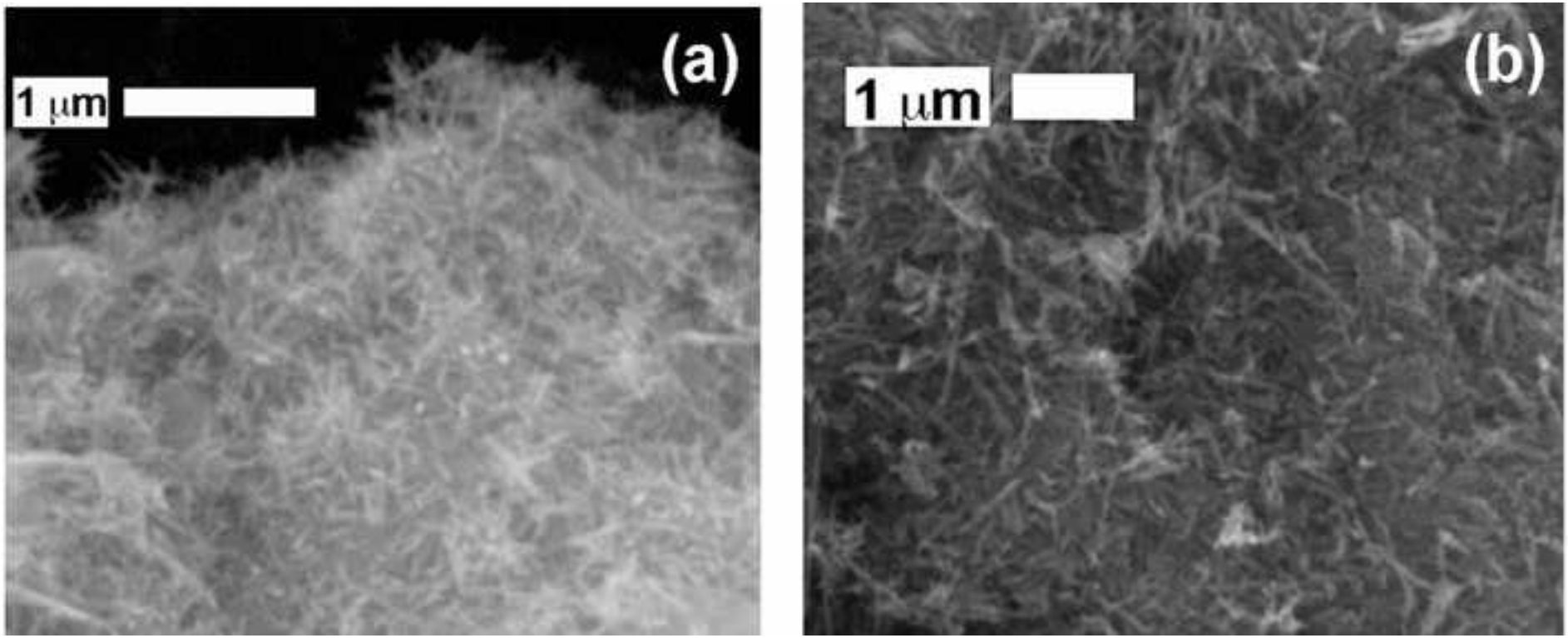

Figure 12

Click here to download high resolution image

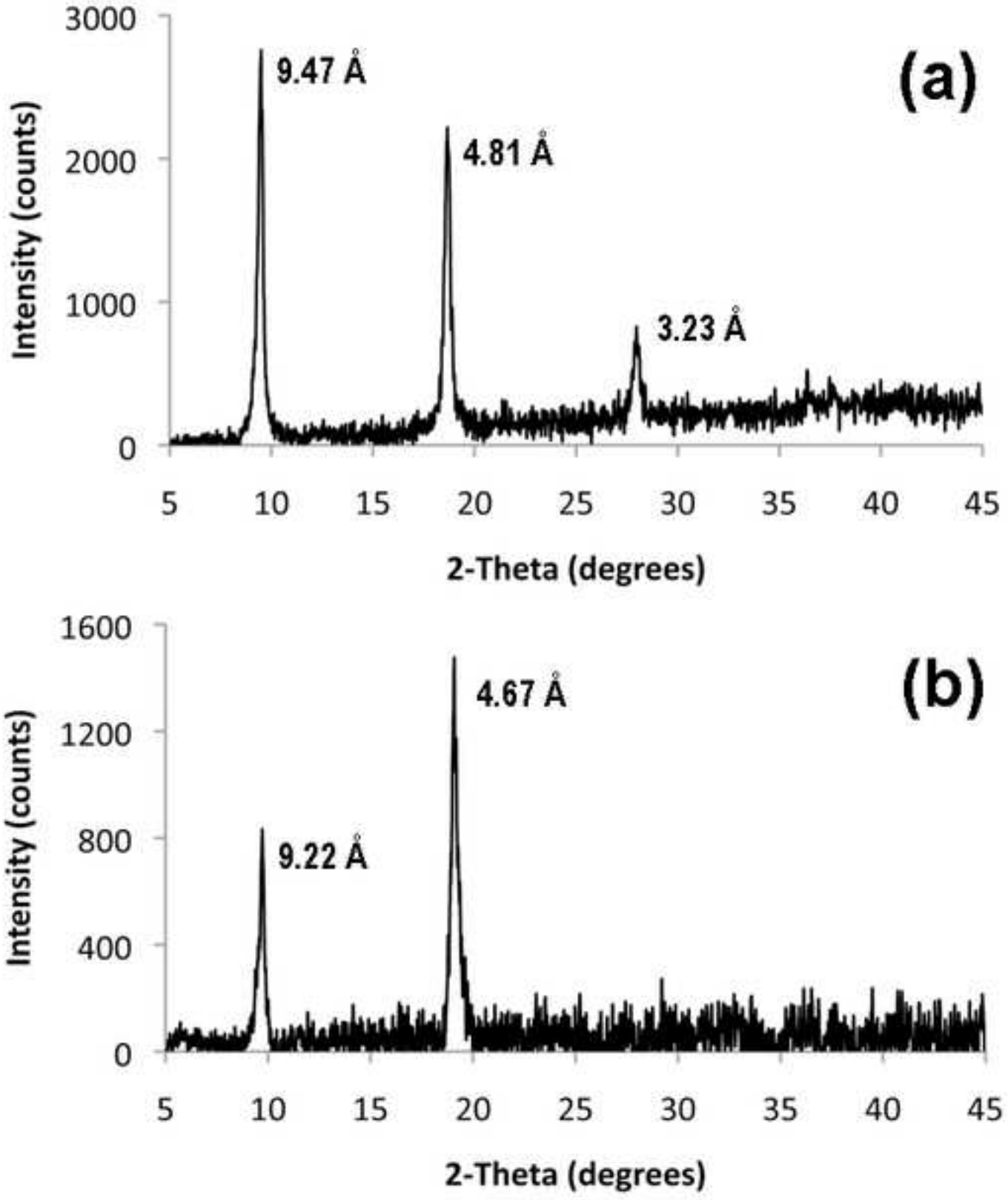

Figure 13

Click here to download high resolution image

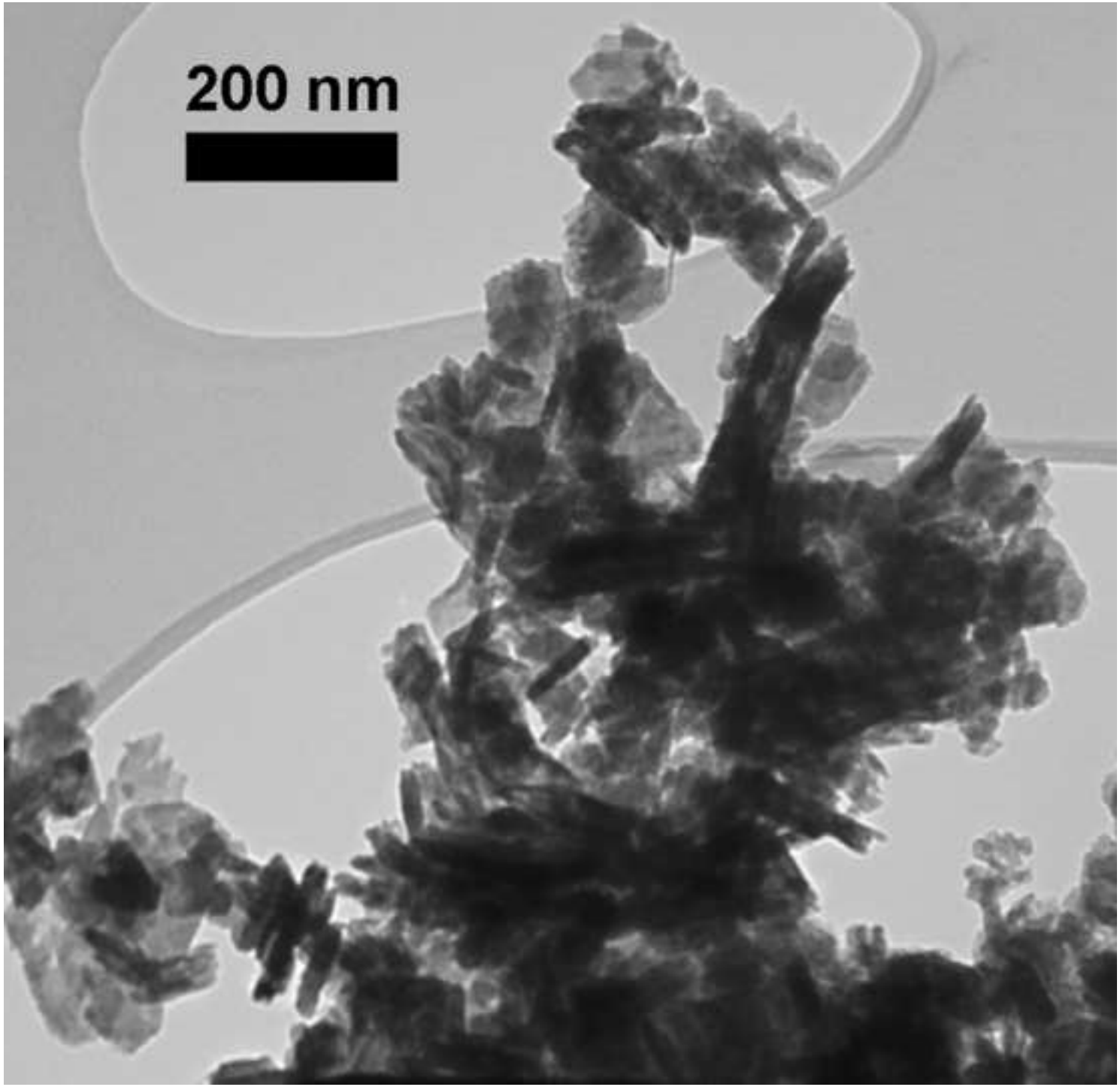

Scheme 1

Click here to download high resolution image